DRY GALLOPING CHARACTERISTIC AND VIBRATION CONTROL OF INCLINED STAY CABLE

Tomo Tanaka[+1], Masaru Matsumoto[+2], Hiroshi Ishizaki[+3], Hiroshi Kibe[+4]
[+1]SE Corporation, Tokyo, Japan
[+2]Kyoto University, Prof. Emeritus, Kyoto, Japan
[+3]SE Corporation, Vice President, Tokyo, Japan
[+4]SE Corporation, Tokyo, Japan

The rain and wind induced vibration (RWIV) and the dry galloping (DG) of the stay cables of cable-stayed bridges are greatly concerning issue for their safety. A numerous studies have been carried out to clarify their generation mechanism and to aerodynamically stabilize those. Recently the authors [1] pointed out that extremely complex RWIV and DG might be excited by the unsteady behavior of the separation bubble (SB) on the cable surface, it means its formation and its destruction (burst) at the particular situations, such as the water rivulet location, the intensity of the axial flow in a near wake of an inclined cable and the critical Reynolds number regime, in similar with the airfoil-stall. Their aerodynamic instabilities are called as stall-type galloping (STG). Based upon this scenario on the generation mechanism, the positive promotion of flow separation to interrupt the formation of SB might effectively stabilize RWIV and DG. The wind tunnel tests have been, in consequence, conducted by the use of rigid cable model with the proto-type size in diameter by installing the large size double helical fillets to verify for their aerodynamic stabilization effect. Furthermore, DG mechanism at the critical Reynolds number regime of the non-yawed cable has been investigated in comparison of the stationary and fluctuating lift forces and the stationary drag force with the cross-flow response of the both cases of non-yawed cable and the yawed cable without/with the double helical fillets.

Keyword: stall, dry galloping, double helical fillet, full scale cable model, aerodynamic stabilization

1. INTRODUCTION

The rain and wind induced vibration (RWIV) and the dry galloping (DG) have been widely known to be typical aerodynamic vibrations of the inclined stay cable of the cable stayed bridge. The numerous investigations also have been carried out, however the precise generation mechanism hasn't been clarified, because of their extremely complex and sensitive fluid-structures interaction mechanism in relation to the water-rivulet on cable surface, the axial-flow in a near wake and the Reynolds number.

The authors [1] have recently pointed out the substantial role of an unsteady production/burst of the "Separation Bubble (SB)" which were generated by the separation and reattachment of the flow on a cable surface for excitation of RWIV and DG, similarly with airfoil-stall [2]. They have called it the "Stall-Type Galloping (STG)", since that fluid phenomenon is fundamentally identical to the airfoil stall. Rinoie [2] has pointed out that the definitely essential role of the behaviour of the separation bubble on the airfoil at near the stalling critical angle, in particular, the appearance of the low frequency fluctuation of flows and lift force at the critical stall event related to K-H instability. It should be noted that the low frequency fluctuation of flow and lift force at the critical stall event must be a key issue for the detection of stall events.

Based upon this scenario on the generation mechanism, the positive promotion of flow separation to interrupt the formation of SB might effectively stabilize RWIV and DG. The wind tunnel tests have been, in

[+1]tomo_tanaka@se-corp.com, [+2]matsu@brdgeng.gee.kyoto-u.ac.jp, [+3]hiroshi_ishizaki@se-corp.com, [+4]hiroshi_kibe@se-corp.com

consequence, conducted by the use of rigid cable model with the proto-type size in diameter by installing the large size double helical fillets to verify for their aerodynamic stabilization effect. Furthermore, DG mechanism at the critical Reynolds number regime of the non-yawed cable has been investigated in comparison of the stationary and fluctuating lift forces and the stationary drag force with the cross-flow response of the both cases of non-yawed cable and yawed cable without/with the double helical fillets. In summary it has been clarified that the double helical fillets with big size can sufficiently stabilize DG of the non-yawed and yawed cables without increasing the drag force. Furthermore, the generation mechanism of STG, that is DG at the critical Reynolds number regime, has been investigated in comparison of the stationary and fluctuating lift forces and the stationary drag force with the cross-flow response of the both cases of non-yawed cable and yawed cable without/with the double helical fillets, taking in to account of the low frequency fluctuation of lift force.

2. WIND TUNNEL TESTS

(1) The wind tunnel and the test facilities

This test, in a high velocity wind tunnel of Japan Aerospace Exploration Agency (JAXA) (2mx2m Low Speed Wind Tunnel, H2m×W2m), was carried out in the range of wind velocity up to 36 m/s ($Re=4.8\times10^5$ defined by cable diameter D of 0.2m). The tested flow is a uniform flow ($Iu < 0.1\%$).

The test was carried out at the reconstructed part with the ceiling, the floor and both side walls made of woods in the length of 5m as shown in Photo 1.

At the both wooden walls of wind tunnel, a circular opening was provided for non-preventing the axial flow in a near wake referred to the previous study [3]. Both ends of the cable models are arranged to be positioned at the outside of wind tunnel through these openings. The load-cells or the non-contact displacement meter was set up at the both cable ends and upstream end for measurement of the aerodynamic force and for measurement of the cross-flow response, respectively. And, in free vibration tests, all materials such as a coil spring and a fixed piano wire had also been installed at the outside in the same way. The overview of the wind tunnel facility is shown in Photo 1.

Photo 1: JAXA 2m×2m Low Speed Wind Tunnel

a) Aerodynamic force measurement test

In the aerodynamic force measurement test, the drag force and the lift force were separately measured by the load cell (KYOWA: LTZ-100KA) directly connected to the axial rods of cable model at the both ends. (See Photo 2(a))

The opening of the both side walls were closed in the case of the yawed angle $\beta=0°$ and opened (3D size circle) in the case of the yawed angle $\beta=45°$, respectively.

b) Free vibration test

In the vibration test, the rocking system with the one-degree-of-freedom was adopted in order to prevent of mixing of the rolling type vibration and the structural damping was minimized as much as possible. In particular, the cable-end at the downwind side was fixed by five piano wires as a pin support, and the other cable-end at the windward side is supported by upper and lower four springs.

The amplitude of the cross-flow response was measured by the laser displacement meter (Keyence: IL-600) at the free end. The detail of cable specimen end is shown in Photo 2(b).

The opening of the both side walls were closed as much as possible in case of the yawed angle β=0°. On the other hand, in case of the yawed angle β=45°, the opening was opened (3D circle) to generate an axial flow in the near wake.

(a) Aerodynamic force measurement tests (b) Free vibration tests

Photo 2: The detail of cable specimen end

(2) The cable rigid model and the installed large-size fillets

The cable rigid model of an aluminum tube with polyester coating was used (outer diameter 200mm, thickness 5mm, total length 3200mm). By the roughness measurement of the coating surface, roughness of the polyester coatings was confirmed to have a relatively close value as polyethylene.

Fillets used for this verification are the double helical type, the winding pitch was set to 5.44D (D: cable outer diameter, winding angle: 30° to the cable axis). The fillet cross sections are set to three kinds of shapes (I-type, Circular-type and Square-type (see Fig.1)), the basic height were set at 5, 8, and 10% of the cable diameter D.

The yawed angle β of the cable model was changed in two cases of 0° and 45° with respect to a perpendicular direction from the cable-axis to the wind direction. The cross-sectional shape of the 10% fillet is shown in Figure 1 and a cable model set up for measurement with I-type fillet is shown in photo 3.

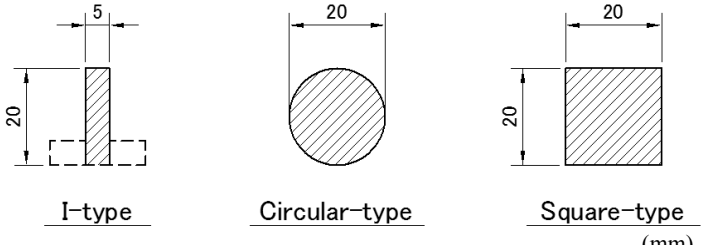

Figure 1: The cross-sectional shape of the 10% fillet

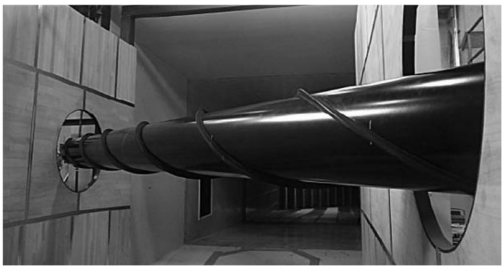

Photo 3: A cable specimen with I-type fillet

(3) Vibration characteristics

The vibration characteristics of 1 DOF locking system, at V=0 m/s, (V: Oncoming wind velocity) are as follows: the frequency is approximately 1.3Hz and the logarithmic decrement was approximately $1.2\sim1.4\times10^{-3}$ at the amplitude of 10mm. The mass per unit length of cable model was 25.8 kg/m, the mass rocking inertia was 202.2 kg·m2, Scruton number of 1DOF locking system was approximately 70.8 (equivalent corresponding Scruton number of heaving vibration is 1.4).

4. AERODYNAMIC FORCE MEASUREMENT TEST

(1) Drag force measurement

The drag coefficient calculated from results of the drag measurement is shown in Fig. 2. The drag coefficient C_D of all test cases was calculated from the following equation.

$$C_D = \frac{F_D}{0.5 \cdot \rho \cdot V^2 \cdot D}$$

F_D: the drag measured by load-cell per unit length [N/m], ρ: Air density [kg/m^3],
V: Wind velocity [m/sec], D: Cable diameter [m]

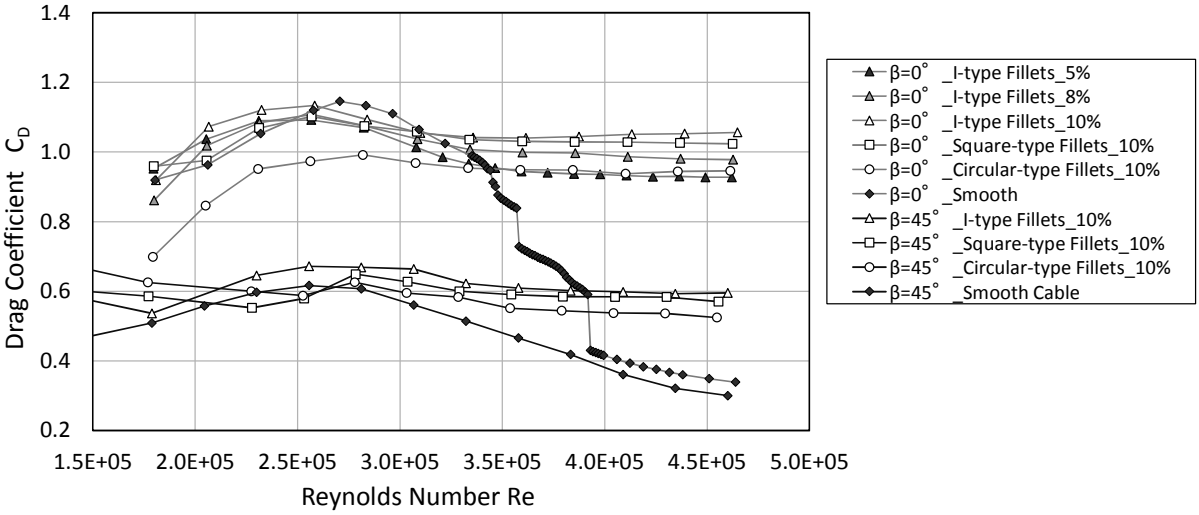

Figure 2: Characteristics of the drag coefficient C_D in terms of the Reynolds number Re

a) Drag coefficient C_D v.s. Reynolds number Re of the Smooth cable at the yawed angle β=0°

The drag-crisis at around Re=3×10^5 ~4×10^5 was observed as shown in Fig.2. The characteristics of the drag-Reynolds number show almost similar property reported by Schewe [4]. It should be noted that at the extremely narrow range of the Reynolds number and at the slightly bigger than Re=3.5×10^5, the slight discrete change of drag. Describing the details on the drag crisis, in the result of Schewe [4], only one drag-crisis appears, on the other hand, twice or thrice drag-crises are observed at slightly bigger than Re=3.5×10^5, and the around Re=3.7×10^5 and 4.1×10^5. This different property is thought to be caused slight change of flow fields caused by various different test conditions. On the other hand, Liu [5] showed the twice drag-crises at near Re=3.5×10^5 and at near Re=4.3×10^5. As far as the magnitude of C_D, at the prior drag-crisis and at the sub-critical Reynolds number regime, C_D ≈1.2, which almost with agree with the test results by Schewe and Liu. On the other hand, at the post drag-crisis and at the super critical Reynolds number regime, there is discrepancy of C_D. C_D in this study shows a little less than 0.4 and gradually decreasing with increase of the Reynolds number, which might be roughly identical with Liu's result. But Schewe'case shows C_D ≈2.5 and almost constant with increase of the Reynolds number. The reason of this significant difference of C_D at the super-critical Reynolds number is not cleared, so further survey on this point is needed.

b) The fillet effect on C_D of the non-yawed cable (β=0°)

C_D of I-type 10% fillet and Square-type 10% fillets were C_D ≈1.1 at the maximum at the sub-critical Reynolds number regime. It should be noted that the installation of big size fillets do not increase C_D at the subcritical Reynolds number regime less than 3.25×10^5. At the Reynolds number regime larger than 3.25×10^5 C_D shows around 0.9 ~1.1 in the different cases of different fillet shape and the fillet height. At this higher Reynolds number regime, the fillets increase C_D than the smooth cable, but from the point of view of the wind resistance design of the stay cable, this property is not concerned matter, because of utilization of C_D at the subcritical Reynolds number regime for the evaluation of wind load on the stay cables.

c) Drag coefficient C_D characteristics at the yawed angle β=45°

In the yawed angle β = 45°, C_D of the cable without/with fillets remarkably decreased in comparison with the result of β=0°. C_D is decreased to approximately 0.6 from 1.1 with Re=around 3.0×10^5.

In the case of the smooth cable, C_D gradually and mildly is decreased at the range of between Re=2.7×10^5 and Re=4.8×10^5. This C_D mild decreasing property might be a kind of drag-crisis, which would excite STG, that is cross-flow response (Katsuchi [6], Andersen&Jakobsen [7]). The installation of fillets can eliminate the mild drag-crisis as shown in Fig.2, it is, in consequence, expected that the DG would be stabilized.

(2) Lift force measurement

Lift coefficient calculated from results of the lift force measurement is shown in Fig.3. The lift coefficient C_L of all models was calculated from the following equation.

$$C_L = \frac{F_L}{0.5 \cdot \rho \cdot V^2 \cdot D}$$

F_L: the lift measured by load-cell per unit length [N/m], ρ: Air density [kg/m^3],
V: Wind velocity [m/sec], D: Cable diameter [m]

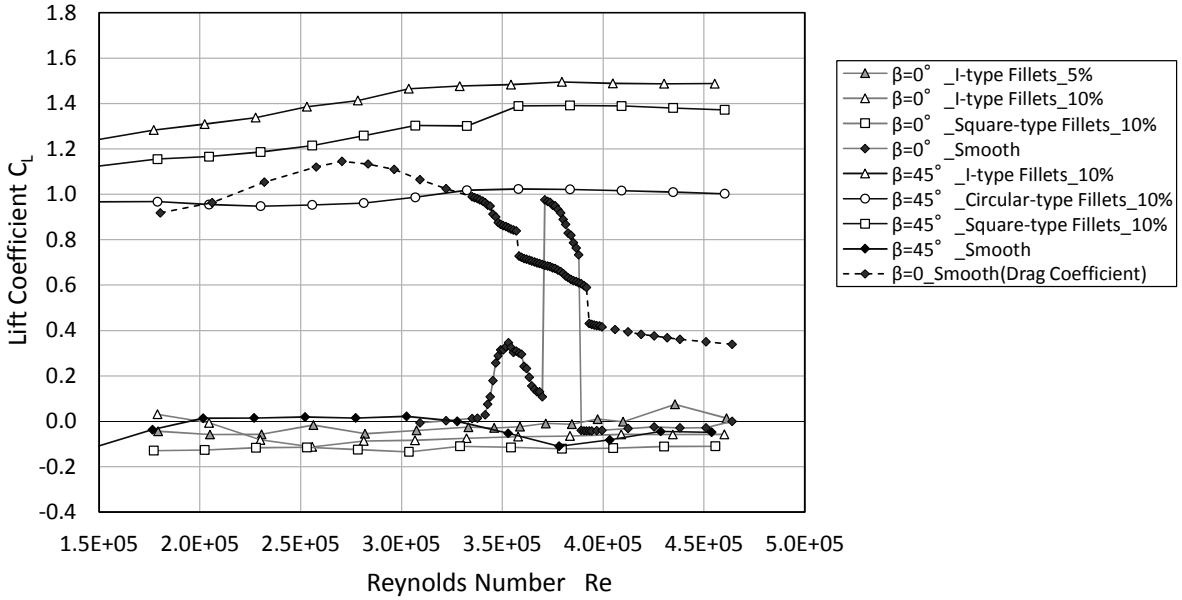

Figure 3: Characteristics of the lift coefficient C_L and the Reynolds number Re

a) Lift coefficient C_L of the non-yawed (β=0°) smooth cable

Former studies [4], [5], [8], [9], it was verified that steady lift of the non-yawed (β=0°) smooth cable, was produced at the critical Reynolds number regime. Which must be caused by the formation of the separated bubble on one side face of circular cylinder. Furthermore, it is also known that the generation of the steady lift is highly correlated with the drag crisis at the critical Reynolds number regime. However the particular Reynolds number regime where the steady lift is generated, are different among the related previous literatures, because of the extremely sensitive flow at the particular critical Reynolds number, where the stall might occurs, affected by many test conditions. As far as the peak value of stationary lift coefficient, Schewe [4], Larose [8], Benidir&Flamand [9], Liu [5] reported C_L≈1.1, 0.8, 1.1~1.4, and 1.6, respectively. This test result shows C_L≈1.1.The significant different characteristics of the stationary lift at the critical Reynolds number regime from the previous test results are twice or thrice appearances as in shown in Fig.3. As described above, the delicate discrepancy of the force characteristics at the critical Reynolds number regime might be caused by the difference of various tests condition. C_L shows almost zero at the outside of the critical Reynolds number regime where the drag-crises and the stationary non-zero C_L have been observed similarly with the previous test results by Schewe [4], Benidir&Flamand [9], Liu [5].

b) The fillet effects on C_L of the non-yawed(β=0°) cable model

C_L of the non-yawed cable (β=0°) with fillet seems to be fundamentally almost zero.

c) Lift coefficient C_L characteristics at the yawed (β=45°) cable without/with fillets

C_L at yawed angle β=45° was approximately 1.0 ~1.6 with gradual decrease with the Reynolds number as shown in Fig.3 because of unsymmetrical geometrical shape caused by the existence of helical fillets associated the cable center in the wind tunnel test section. On the other hand, C_L of the yawed (β=45°) smooth cable is almost zero at the Reynolds number of (1.5~5.0) $\times 10^5$ as shown in Fig.3.

5. FREE VIBRATION TEST

(1) Cross-flow response characteristics of the non-yawed (β=0°) cable

a) Smooth cable

The non-yawed (β=0°) smooth cable without fillets showed velocity restricted response at the multiple velocity ranges as shown in Fig.4 in correspondence to observation of the multiple drag-crises, explained above. It was significantly interesting that those responses were observed at the particular wind velocity range where the drag-crises and the stationary lift force occurred, even though the complete different tests, those are stationary test for force measurement of the stationary cable model and the vibration test in the 1DOF locking system. In the detail, the cross flow response seems to appear at the wind velocity correspondingly to the disappearance of stationary lift caused by the destruction (burst) of the separation bubble. On the other hand, Liu [4] reported the cross flow velocity restricted response appears correspondingly to the both velocity where the of the stationary lift starts disappears.

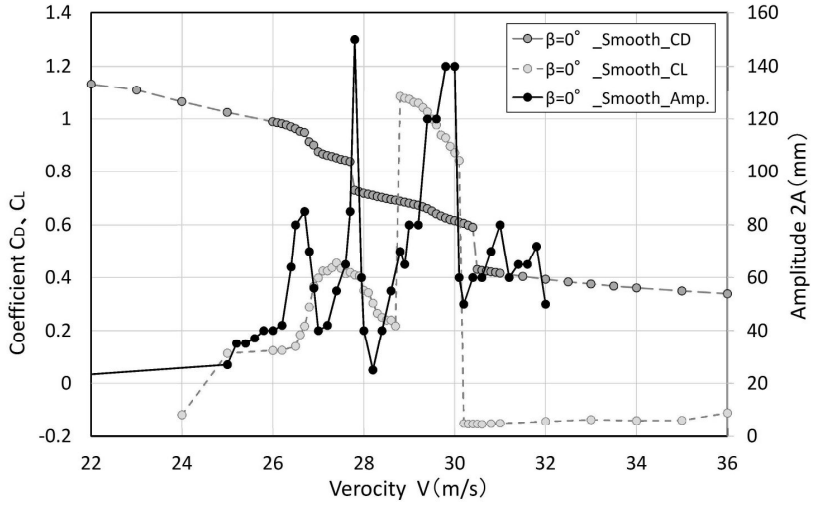

Figure 4: 2A-V diagrams of the smooth cable at the yawed angle β=0° with C_D,C_L

b) PSD of the unsteady lift force at the low frequency range of the non-yawed (β=0°) smooth cable

In order to verify the generation mechanism of these velocity-restricted response of non-yawed (β=0°) cable, the PSD (Power Spectral Density function) at the low frequency regime, less than 5Hz. As explained before, the stall phenomenon should produce the low frequency fluctuation of velocity around an obstacle, in another expression, the stall phenomenon can be detected by the existence of the low frequency fluctuation of velocity or lift force, therefore PSD of the lift force at the low frequency regime was analyzed at various velocity where cross flow responses were observed as shown in Fig.5. As shown in Fig.5, the typical power characteristics in PSD of the lift force at the low frequency regime were observed at correspondingly to the velocity where the cross-flow response disappears. These PSD properties at the low frequency caused by the stall are similar with those at the stall of a circular cylinder at the particular critical Reynolds number studied by Schewe [4], a circular cylinder with protuberance at the particular position of 50° from the front stagnation point at the subcritical Reynolds number regime studied by the authors [1], yawed (β=45°) circular cylinder, snow-accreted conductors studied by Matsumiya [10]. At slightly increase of velocity, it is finishing of the cross-

flow response caused by the stall, the low frequency fluctuation of lift force cannot be observed as shown in the left and bottom Fig.5 (velocity of 30.2m/s). In summary, the cross-flow response of the non-yawed cable might be a kind of STG.

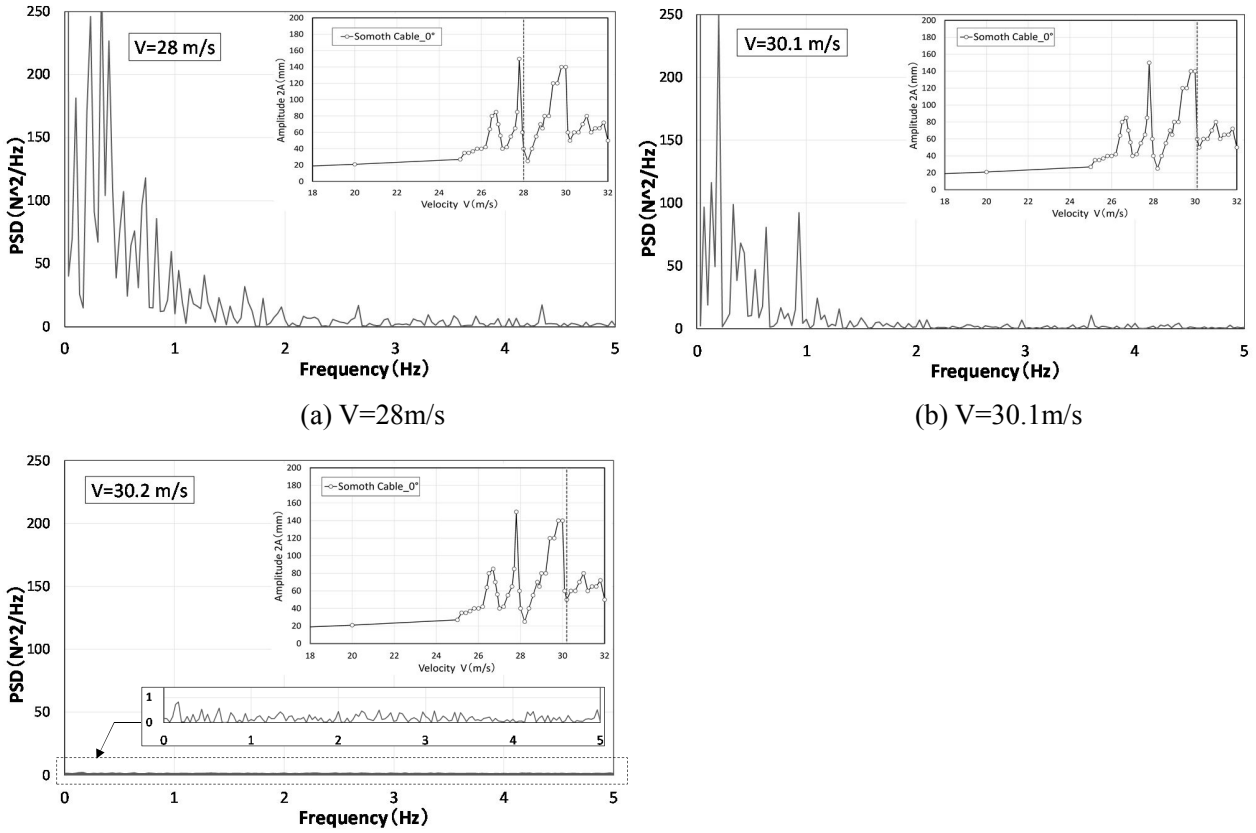

(a) V=28m/s (b) V=30.1m/s

(c) V=30.2m/s

Figure 5: P.S.D of the lift force of the smooth cable at the yawed angle β=0°

(2) Cross-flow response characteristics of the yawed (β=45°) cables

a) Smooth cable

Saito [11], Kimura [12] and Matsumoto [3] have reported the cross-flow response of the yawed (β=45°) circular cylinder, separately. In particular first two studies, the tested Reynolds number was covered in the both regimes of the sub-critical and the critical. All of the responses in three test results started at the reduced velocity Vr (=V/fD) of approximately 40, or 50. However, in the first two test results, the amplitude of cross-flow response becomes small or stabilized at the particular Reynolds number of $Re=1.5\times10^5$~2.0×10^5. At the high Reynolds number, that is the critical Reynolds number, the particular low frequency vortex must be generated by the stall by the axial flow, but the different more intensive vortex might be produced by the critical Reynolds number. On the other hand, the cross-flow response measured in this study continues the divergent-type response after the onset without locally stabilized in the other two tests results, as shown in Fig.6. The authors evaluate that the two sorts of response are excited by the stall caused by the axial flow at the subcritical Reynolds number and the one by the critical Reynolds number, respectively. The locally stabilized response at the particular high Reynolds number might be caused by the intensive interaction of an intensive vortex generated by the low frequency fluctuation of the flows related to the stall. The reason, why the response does not show the locally-stabilized property, is thought to be caused by the extremely small Scruton number of the 1DOF rocking system. The switching property of the stall-mechanism, latently hidden in the divergent-type response diagram shown in Fig 6, can be detected by the analysis of the low frequency property of the PSD of the lift force as lately explained.

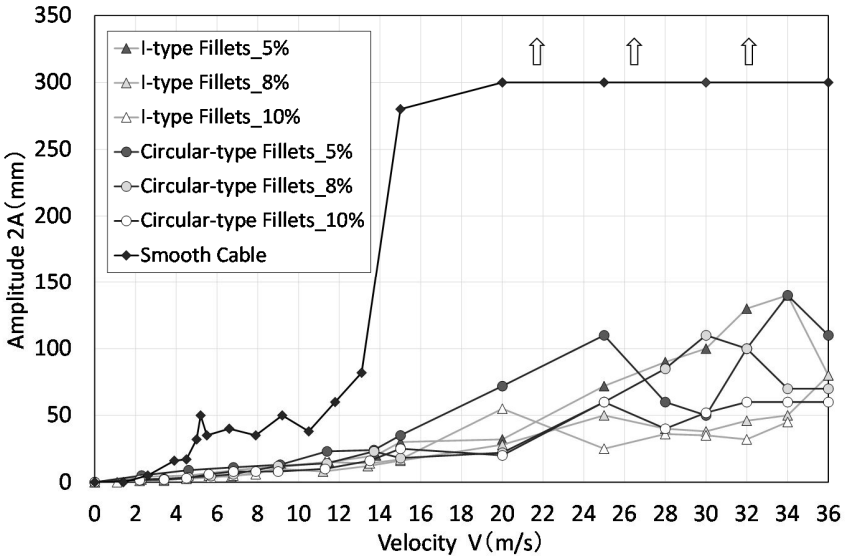

Figure: 6 2A-V diagrams of the smooth cable and the cable with fillet at the yawed angle β=45°

b) Fillet effect on the yawed (β=45°) cable

The cross flow response of the yawed (β=45°) smooth cable can be drastically stabilized by the installation of the proposed large size double helical fillets with various shapes and various size of 5%,8% and 10%as shown in Fig. 6. The response at the higher velocity shows a random vibration induced by the amplified flow separation by the helical fillets. The proposed large size helical fillets can be significantly stabilize the cross flow vibration, that is the dry galloping as a type of stall galloping(STG) even though under the extremely small Scruton number.

c) PSD of the unsteady lift force at the low frequency regime of the yawed (β=45°) smooth cable

As described above, to detect the latent switching of the stall mechanism by the axial flow and the critical Reynolds number, the PSD analysis of the unsteady lift force, at the low frequency regime, of the yawed (β=45°) smooth cable measured by the force-measurement tests at various wind velocities. At the low velocity regime of V=12m/s~20m/s, where the cross-flow response appeared, significantly small power at the low frequency regime of unsteady lift force were observed, however, at the higher wind velocity than V=24m/s ($Re=3.2\times10^5$) approximately, its power drastically becomes large. Fig.7 shows the examples of their PSDs at V=18m/s, 24m/s and 29.6m/s. Thus, the switching of stall mechanism might be occurred at V≈24m/s. The cross flow response at the higher velocity regime than V≈24m/s might be generated by the stall related to the critical Reynolds number.

d) Aerodynamic stabilization by the large-size double helical fillets

Taking into account that the RWIV and DG of the inclined cable, and they must be Stall-type galloping essentially related by the separation behavior characterized unsteady flow change between the separated flow and the reattached flow, the large-size double helical fillets were investigated with the expectation of the mitigation of the stall appearance by the promotion of flow-separation by the large-size object on cable-surface. As in shown in Fig.6, the cross-flow divergent-type violent response of yawed (β=45°) was drastically stabilized by the helical fillets. As shown in Fig.7, in the PSD of lift force at the low frequency of the yawed (β=45°) cable with the double helical I-type fillets at the all wind velocities regime between V=12m/s and 36m/s, the significant power at the low frequency regime is not observed. (See the example of the case of V=30m/s in Fig.7.) Thus it is verified that the large-size fillets must prevent the stall and stabilize the sequential aerodynamic instability. Furthermore, it is verified that the power-property in the PSD diagram of the lift force at low frequency is a key-property of the stall of various bodied including an airfoil with the critical stalling angle.

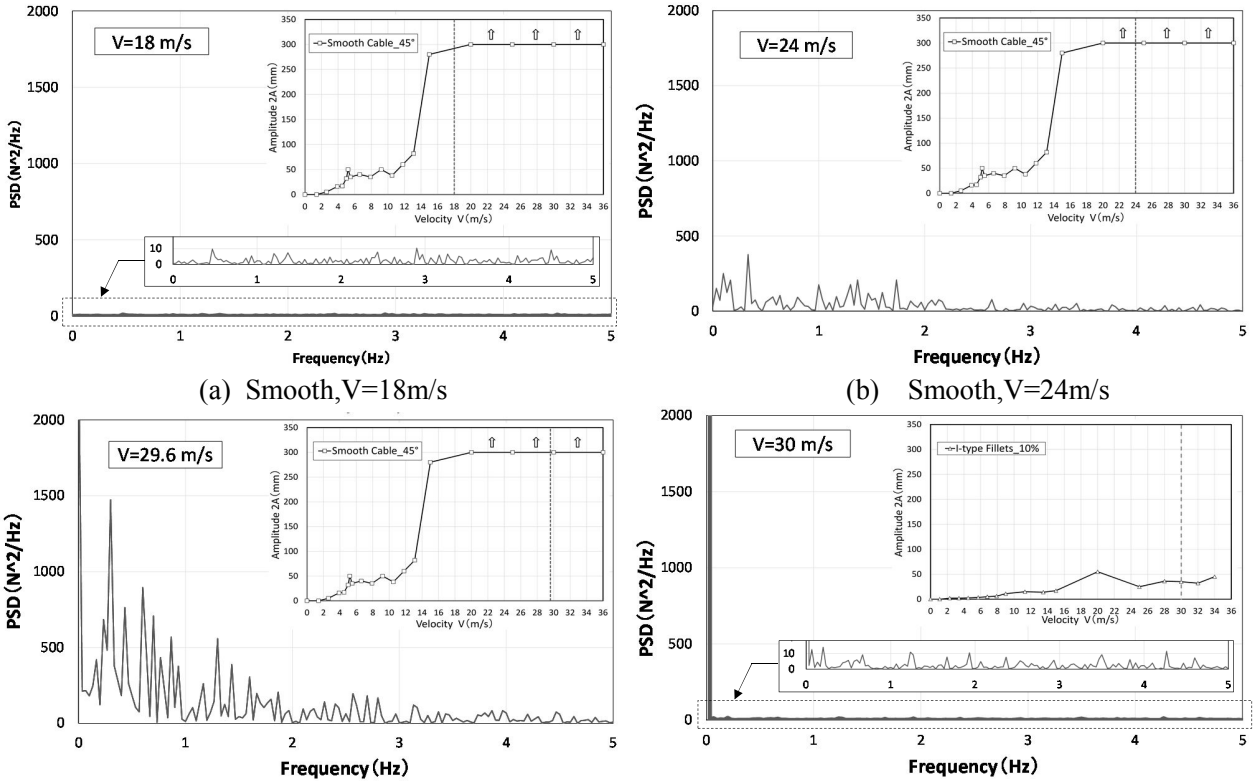

(a) Smooth,V=18m/s (b) Smooth,V=24m/s

(c) Smooth,V=29.6m/s (d) I-type fillet_10%,V=24m/s

Figure 7: P.S.D of lift force of the smooth cable and the cable with I-type fillet at the yawed angle β=45°

6. CONCLUSION

The main conclusions obtained in this study are as follows:

(1) Drag force

The drag force of the cable installed of the big-size double helical fillets is almost identical with the smooth cable at the sub-critical Reynolds number of approximately $C_D \approx 1.1$. Furthermore, the drag force of the cable installed of the big-size double helical fillets does not show the drag-crisis, which is observed for the smooth cable at the critical Reynolds number regime, and sustain the almost same value at this high Reynolds number regime. The drag crisis of the non-yawed (β=0°) smooth cable is observed roughly similar with the result formerly studied by Schewe [4], but in details, the two times or three times multiple drag-crises were observe in this study. On the other hand, in the case of C_D of yawed (β=45°) smooth cable, the gradual decrease of C_D at the comparatively high Reynolds number regime is thought to be a kind of drag-crisis similarly reported by former studies(Larose [8], Katsuchi [6], Georgakis[13]).

(2) Stationary lift force

The stationary lift force is observed at the particular multiple Reynolds regime in corresponding well to the appearance of the drag-crises in relation to the formation or destruction of the separated bubble on the cable-surface. The maximum value of the stationary lift coefficient, C_L, is $C_L \approx 1.1$, which is roughly identical or smaller than those reported by Flamand [9] and Liu [5], respectively.

(3) The cross-flow response of the non-yawed (β=0°) smooth cable

The cross-flow response of the non-yawed (β=0°) smooth cable is observed, in well correspondingly, at the particular wind velocity/Reynolds number regime where the drag-crises appeared. These responses seem to appear when the response disappear.

(4) The cross-flow response of the yawed (β=45°) smooth cable and the one of the cable with a large-size helical fillets

The yawed (β=45°) smooth cable showed the violent divergent-type cross-flow response is observed similarly with the former test results. The onset reduced wind velocity, Vr=V/fD, was evaluated to be approximately 40~50 in similar with test results by Saitou [11], Kimura [12] and Matsumoto [3]. After installation of the large-size double helical fillets, the violent divergent-type cross-flow response can be drastically stabilized even though the random response with small amplitude remains at higher wind velocity.

(5) The reappearance of the stall-type galloping

It is verified that the stall-appearance of the dry galloping of non-yawed (β=0°) cable at the critical Reynolds number regime and the one of yawed (β=45°) at the wide Reynolds number regime including the subcritical and the critical Reynolds number, can be detected by the PSD-property of the unsteady lift force.

(6) The stabilization effect of the large-size double helical fillets

It is verified that the proposed the cable with large-size double helical fillets shows significantly stable against the dry-galloping of stay cable, and also against the rain and wind induced vibration(RWIV) because of the interruption (Ueshima [14]) of the formation of the upper water rivulet without the increase of drag force on the stay cables.

ACKNOWLEDGEMENT

The authors would like to express the deepest appreciation to Mr. H. Inoue (NIPPON KAIJI KYOKAI(ClassNK), ex-MES), Mr. Y. Miyasaka (Miyasaka Co.), Dr. J. Nakamichi (JAXA), Dr. K. Saito (JAXA) and Dr. H. Arizono (JAXA) for their worthy advises on these wind tunnel tests.

REFERENCES

1) Matsumoto, M., Ishizaki, H. : Stall-type Galloping and VIV-initiated Galloping of Inclined Stay Cable Aerodynamics and its Aerodynamic Stabilization. Proc. of SDAC, Lyngby Denmark, 2014.
2) Rinoue, K. : “Laminar separation bubbles formed on airfoils”, NAGARE(Fluid) 22, pp15-22, 2003 (in Japanese)
3) Matsumoto, M. : The role of Axial Flow in Near Wake on the Cross-Flow Vibration of the Inclined Cable of Cable-stayed Bridges, Proc. of FIV Symposium, Montreal, 2010.
4) Schewe, G. : On the force fluctuations acting on a circular cylinder in crossflow from subcritical up to transcritical Reynolds numbers, JFM, 265-285, 1983.
5) Liu, K., Wang,Y., Cheng,Y., Ma,W. : Reynolds Number Effect on Wind-Induced Vibration of Stay-Cables Proc. of the 9th ISCD, Shanghai, China, 2011.
6) Katsuti,H, Yamada H.: Dry galloping characteristics of indented stay cables in turbulent flow, Proc of 7th ISCD, Shanghai, 2011
7) Andersen,T.,Jakobsen, J.B., Macdonald,J.Nikitas,N., J.Larose,G.,Sarvage,M.,McAulifee,B.G. : Drag crisis response of an elastic cable model, Proc of 10th ISCD, Paris, 2003.
8) Larose, G.L., Savage, M.G.,Jakobsen,B.J.,: Wind tunnel experiments on an inclined and yawed circular cylinder in the critical Reynolds number range, Proc.of 11th ICWE, Lubbock, Texas, 2003
9) Benidir and Flamand,L.Gaillet,G.Dimitriadis “dry galloping on bridge cables: shape effect on an inclined circular cylinder in the wind tunnel” Proc. of the 6th EAWEC, 2013, London,
10) Matsumiya : personal communication.
11) T.Saito : personal communication.
12) Kimura, K., Kato, K., Kubo, K., Ohashi, Y. : An Aeroelastic Wind Tunnel Test of an Inclined Circular Cylinder, Proc. of 8th ISCD, Paris, 2009.
13) Matteoni, G., Georgakis, C., : Aerodynamic coefficients of dry inclined cables in smooth flow, Proc. of the 9th ISCD, Shanghai, 2011.
14) Yamauchi, K., Uejima, H., Kuroda, S., An investigation of the Aerodynamic Characteristics of Cable with Surf ace Ribs, 9th ISCD, Shanghai,2011.